VALIDATION OF THE ARMY BURN TO VIOLENT REACTION (ABVR) TEST AS A TOOL TO PREDICT FULL-SCALE MOTOR RESPONSE TO FRAGMENT IMPACT

#20136

J. B. Neidert, M. A. Pfeil and J. A. Stanfield
Aviation and Missile Research, Development and Engineering Center
Redstone Arsenal, AL

ABSTRACT

While the ABVR experiment has been used rather extensively to investigate the reaction mechanisms of rocket motors subjected to fragment impact, no efforts have been made to validate that it truly represents how a full scale motor, with nitramine-based propellants, would behave under similar circumstances. Thus, efforts are made herein to validate the ABVR experiment by comparing the detonative response it produces to those obtained in cylindrical experiments and analog motors. Results indicate that the ABVR experiment is a valid sub-scale to predict the detonative response of full-scale motors. The insight gained from the ABVR experiments has resulted in a possible new screening tool during the development of new, insensitive compositions.

INTRODUCTION

Since 1989, the Burn to Violent Reaction (BVR) and Army Burn to Violent Reaction (ABVR) experiments have been implemented as a sub-scale experiment that could potentially represent the response of a full scale rocket motor subjected to fragment impact[1-5] Both nitramine and ammonium perchlorate (AP) based propellants have been investigated, and multiple parameters, including case material, propellant thickness, fragment type, fragment velocity, confinement, air gap (spacing between propellant slabs), and backing material, have been found to affect the outcome. In the case of nitramine based propellants, significant insight has been gained into the different detonation mechanisms that could occur inside a rocket motor and what critical parameters control those responses. For AP based propellants, the BVR/ABVR experiments have allowed for mapping of the severity of the reaction, based on a variety of parameters. These findings have been quite useful in understanding the issues and hazards associated with fragment impact.

Given the understanding, the significant reduction in testing costs, and reduction in hazards associated with testing that the BVR/ABVR experiment has provided, it would be very beneficial to validate their accuracy in predicting the actual response of a full scale motor. Some efforts have been made to accomplish this, but they have been limited in scope and have focused on AP based propellants. While those efforts showed promise in validating the BVR/ABVR experiment for AP based propellants, no efforts have been made to validate them for detonable, nitramine-based, propellants.

As such, the focus of the current effort is to address this lack of subscale model validation for nitramine-based propellants. To accomplish this, multiple experiments were conducted using the ABVR setup, and parameters such as fragment velocity, propellant thickness, and air gap were investigated. These experiments were then repeated, but cylindrical sections of simulated rocket motors were used. The ABVR

experiment is validated by comparing its reaction response to that of the cylindrical sections. Further experiments and validation were completed by testing full-scale analog motors and comparing reaction responses.

EXPERIMENTAL METHODS

There were four separate test articles evaluated, including the ABVR experiment, cylindrical sections, and an analog full scale motor (see Figure 1). All experiments used a NATO STANAG 4496 Fragment Simulated Projectile (FSP), made from 1018 carbon steel. The FSP was sabot launched out of a 20 or 40 mm smooth bore cannon and passed through a sabot stripper and three break screens before impacting the test article. For all experiments, except those that used an analog motor, backlighting was provided via a Megga-Flash PF300 Slow Peak Flashbulb placed behind a 1"x1" square grid. For the analog motor tests, the same type of flashbulb was used to illuminate the test article. Multiple high speed Phantom cameras were used it each test to observe the overall reaction (slower frame rate) and the events occurring within the air gap between the propellant (faster frame rate). Images were recorded at a frame rate varying between 75,000-260,000 frames per second.

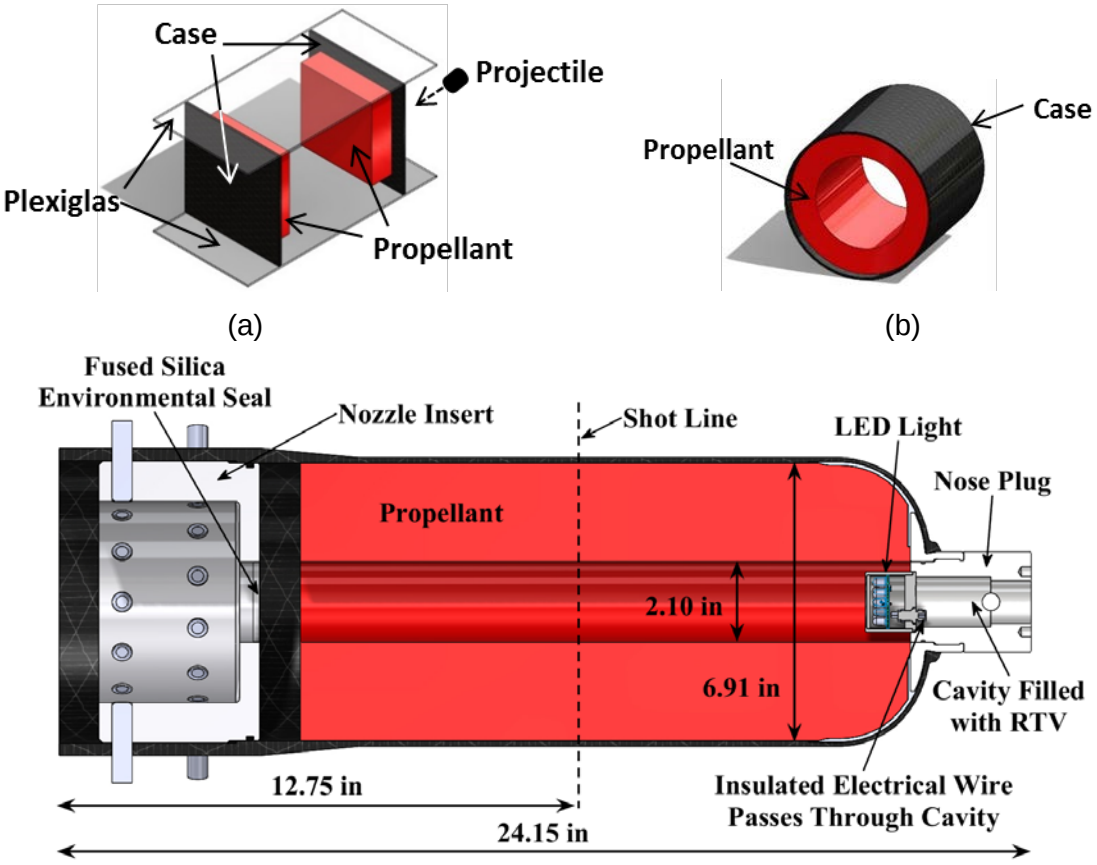

Figure 1 The various test articles used in this effort: (a) an ABVR experiment, (b) a cylindrical section, (c) full-scale analog motor

ABVR AND CYLINDRICAL SECTION

The ABVR test article, see Figure 1 (a), consisted of a 4.5 x 4.5 in square slab of MSP-1 propellant with a thickness of 1.25 or 2.5 ± 0.02 in. These were bonded to a casing material and placed in series, with the propellant slabs facing each other. The distance, or air gap, between the slabs of propellant was fixed by either gluing 0.093 in thick Lexan sheets (6 x 12 in) to the casing material or by attaching ¼ 20 nylon rods in each corner of the casing material. The air gap was set by using four stainless steel spacers of the desired length (tolerances of ± 0.005 in) – spacers were removed before tests. Details of the MSP-1 propellant can be found in previous publications. Fragment hit point was aimed at the center of the test article.

Two different casing materials were used in the ABVR experiments. The first was a 0.135 in thick IM7/8552 composite plate. The other consisted of a 0.10 in thick 7075-T6 aluminum plate that was prepped via grit blasting. After cleaning, a primer (Chemlok 205) layer was applied and then a bonding agent (Chemlok Bonder 234B). A layer of 0.030-0.035 in Kevlar filled EPDM Rubber (EP-701-02) insulation was then applied and cured to produce an aluminum casing plate. Both the composite and aluminum plates were adhered to the propellant using a hydroxyl-terminated polybutadiene (HTPB) liner (filled with carbon black).

Cylindrical sections of propellant bonded inside a composite case [see Figure 1 (b)] were also evaluated. These used the same IM7/8552 composite material with a thickness of 0.132 in. The web thickness was kept relatively constant between 1.038-1.135 in with an average of 1.09 in or between 2.288-2.375 in with an average of 2.34 in. The inner and outer diameters of the propellant varied for different air gaps. For some of the experiments, cylinders were quartered, see Figure 2. The outer diameter of the propellant for these samples was kept constant at 5.2 in for both web thicknesses of 1.09 and 2.34 in.

(a) (b)

Figure 2 Quartered sections of cylindrical test articles used in experiments with a web thickness of (a) 1.09 in and (b) 2.34 in.

Both ABVR and cylindrical section experiments were evaluated using the same setup used in previous ABVR testing. Two rows of PCB Piezotronics pencil gauges for pressure measurements were placed at 45° off the shot line at 5, 9, and 13 ft away from the impact point, see Figure 3.

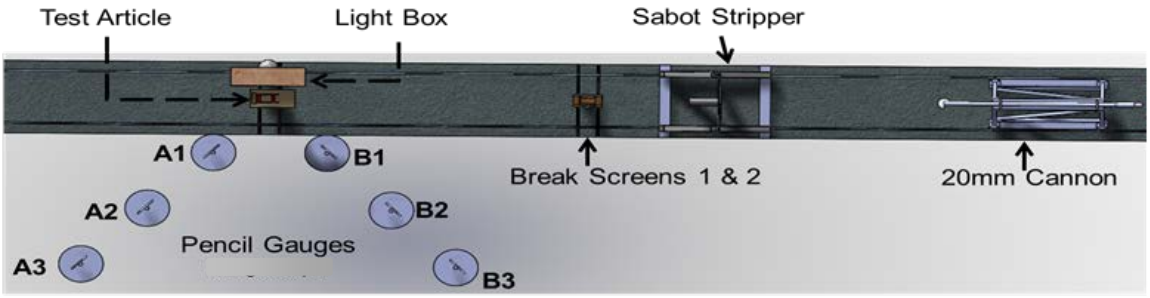

Figure 3 Test setup used to evaluate ABVR and cylindrical test articles.

ANALOG MOTOR

The full scale analog motor, see Figure 1 (c), consisted of a composite case, an aluminum 7075-T73 nozzle insert, and a stainless steel nose plug. The motor had a diameter of 7.18 in and was 24.15 in long. The MSP-1 propellant grain was a 6.91 in diameter cylinder with a 2.10 ± 0.04 diameter center bore perforation, resulting in a web thickness of 2.41 in and a propellant weight of approximately 31.3 lbs. The composite case was 0.135 in thick, at the fragment hit point, and made of IM-7 carbon/epoxy composite with S2 glass layers in the thicker aft closure joint. A layer of Kevlar-filled polyisoprene insulator was at the head end of the motor. An uncoated 1λ fused silica window was inserted into the nozzle to act as a weather seal, provide confinement, and to allow optical access into the motor during testing. A Thorlabs LIUCWHA LED light was placed inside the motor at the head end and was used to illuminate the bore for optical measurements.

The analog motors were placed vertically, nose facing downward, on a 0.5 in thick plywood tabletop with a large enough hole to allow the nose plug to pass through. A 1 x 12 x 24 in steel witness plate was placed beneath the plywood tabletop, 4-4.5 in below the top of the table. A first surface mirror was placed above the motor at a 45° angle to allow a high speed monochrome Phantom camera (recording at 200,000 frames per second) to observed the reactions within the motor. To observe the exact fragment impact point, two grids were placed in line with the vertical and horizontal axis of the fragment shot line at the motor impact point. A high speed monochrome Phantom (recording at 12000 frames per second) camera was used to observe both grids simultaneously. A third high speed color Phantom camera (recording at 6200 frames per second) was used to observe the overall event.

The first two tests had eight and seven evenly spaced PCB Piezotronics pencil pressure gauges placed at a radius of 5 and 10 ft respectively. The second test resulted in a detonation that damaged the pencil gauges located 5 ft away from the test article. The remaining four tests had two rows of pencil gauges placed at 5, 10, 15 and 20 ft behind the test article at 45° offset from the fragment shot line. The shot line was aimed at the center of the motor, 12.75 in from the aft end of the motor.

RESULTS AND DISCUSSION

Three types of reactions were typically seen throughout these tests, including Shock to Detonation Transition (SDT), Unknown Detonation Transition (XDT), and brief combustion events. An SDT event occurs when an insult provides sufficient impulse, over a minimum amount of time, that results in a prompt detonation to occur. In the

present scenario, this insult is provided by the fragment impacting the test article at high speeds, see Figure 4 (a). A detonation event typically commences less than 10 µs after the fragment touches the test article, commencing near the location of the impact point and propagating outwards through the rest of the article. Once a minimum fragment velocity threshold, unique to each test configuration, is achieved, an SDT event will occur. The detonation in both a SDT and XDT reaction results in notable increase in light emission from the test article, pressure measurements that are an order of magnitude or more larger than non-detonation events, and little to no recognizable remains of the test article.

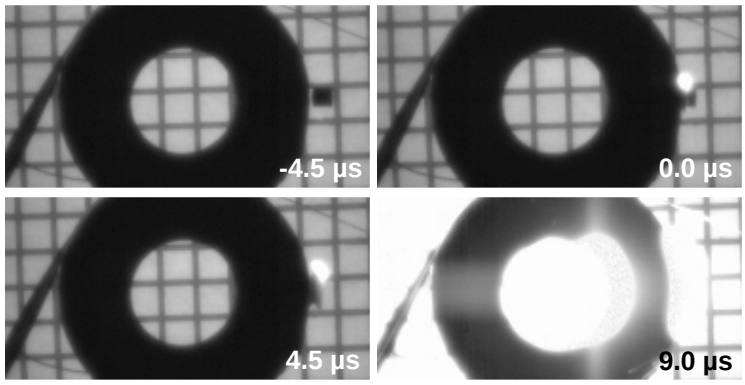

(a)

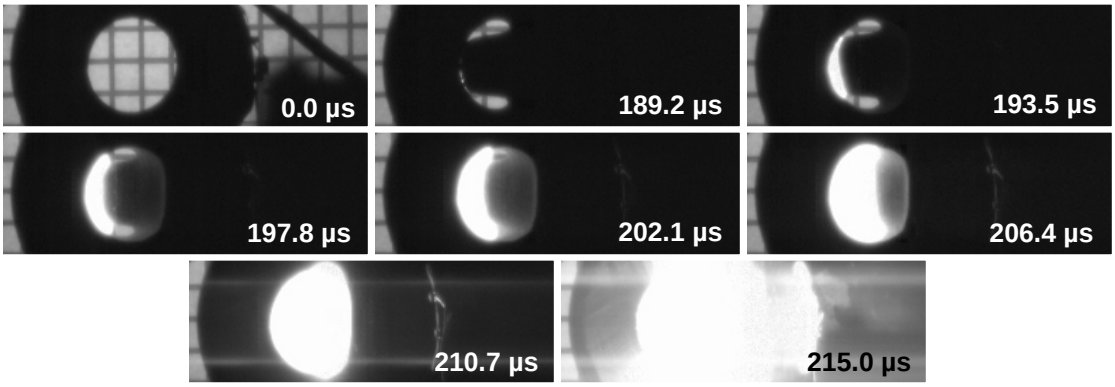

(b)

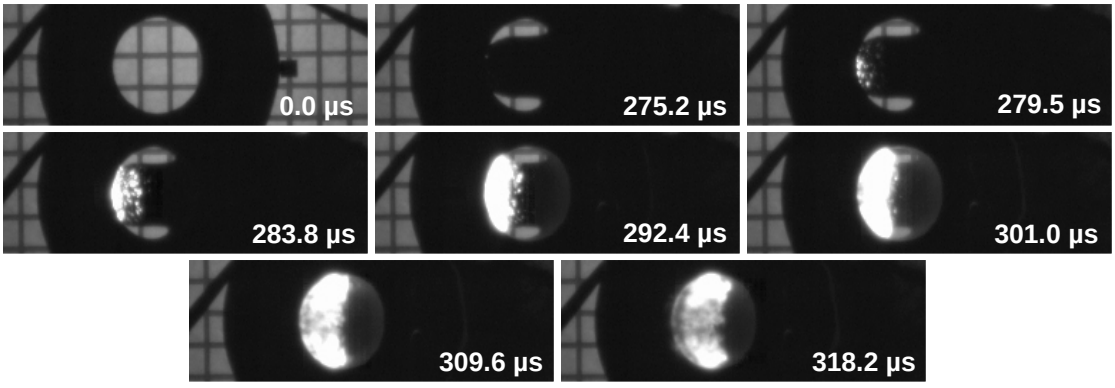

(c)

Figure 4 Still images from three different reaction mechanisms typically observed in these tests: (a) SDT, (b) XDT, and (c) brief combustion.

If the fragment velocity drops below the SDT velocity threshold, then two other types of reactions can occur, XDT or brief combustion. Both reactions result from when the fragment passes through the case and one section of propellant, producing a debris cloud of propellant that propagates across an air gap/bore diameter. Once this propellant cloud impacts the other side of the air gap, it will initiate, and either produce an XDT [Figure 4 (b)] or brief combustion [Figure 4 (c)]. The dynamic properties of the propellant debris cloud control when one or the other reaction will occur. One of the dominating properties appears to be the porosity/continuity of the debris cloud. If the porosity is too low or high, a brief combustion event will occur. If the porosity is in between, a detonation can initiate at the leading edge of the debris cloud and propagate back through the cloud into the undamaged propellant, causing it to also detonate. Such a detonative/brief combustion behavior results in defined regions, dependent on fragment velocity and the test article air gap, where one or the other reaction will occur. This behavior was first noted by Finnegan et al.[1]

ABVR VS. CYLINDRICAL

Comparison of the detonation reactions observed in the ABVR versus what was observed in the cylindrical experiments are provided in Table 1 and Figure 5. The data for the 1.25 in web thickness ABVR samples was obtained from previous efforts reported by Pfeil et al.[5] Table 1 provides the fragment minimum velocity thresholds to produce an SDT reaction; the SDT thresholds are also represented by vertical lines in the plots provided in Figure 5. These thresholds are determined by taking the average velocity of the lowest velocity that produced an SDT reaction and the highest velocity that did not. The SDT thresholds of the ABVR and cylindrical samples, given the same web thickness, are within 334 ft/s or less, a rather minimal difference. Introducing curvature into the experiment causes the SDT threshold to increase slightly for the 1.25 in web thickness but decrease slightly for the 2.50 in web thickness. This discrepancy is likely a result of using quartered, instead of full, cylindrical samples. For the 2.50 in thick samples, detonation reactions were observed to begin on the cut surface, whereas the 1.25 in thick samples were not. Thus, it is likely that the threshold value observed for the quartered 1.25 thick sample is more accurate in representing a non-quartered sample than the 2.50 thick sample.

Table 1 SDT minimum fragment velocity thresholds for ABVR and cylindrical test configurations.

	SDT Threshold, ft/s
ABVR – 1.25 in Web	4329 ± 2
ABVR – 2.50 in Web	4536 ± 125
Quartered Cylinder – 1.09 in Web	4663 ± 63
Quartered Cylinder – 2.34 in Web	4219 ± 104

Both propellant web thickness configurations produced regions where XDT or brief combustion would occur, depending on fragment velocity and air gap. This region of XDT reactions was the same for both ABVR and cylindrical samples that had a web thickness of 1.25/1.09 in, see Figure 5 (a). Doubling the web thickness notably shifted the XDT reaction region and caused the ABVR and cylindrical data to diverge, see Figure 5 (b). Due to the limited data obtained for the ABVR setup with a web thickness

of 2.50 in, the XDT reaction region had to be inferred. The upper air gap limit was determined by the data obtained and by comparing against data provided by Pfeil et al.[5] Their data indicated that using a steel plate, instead of propellant as the surface the debris cloud of propellant impacted, caused the slope of the upper air gap limit line to increase. Based on that observation and comparing against the data they obtained for a 2.50 in web thickness ABVR sample with a steel plate, a likely slop for the XDT upper air gap limit line can be inferred. There was not sufficient data to infer what the XDT lower air gap limit line could be.

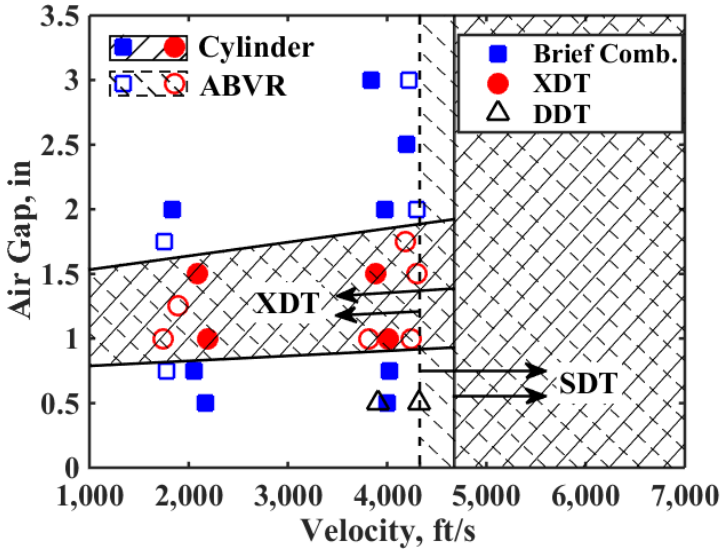

(a)

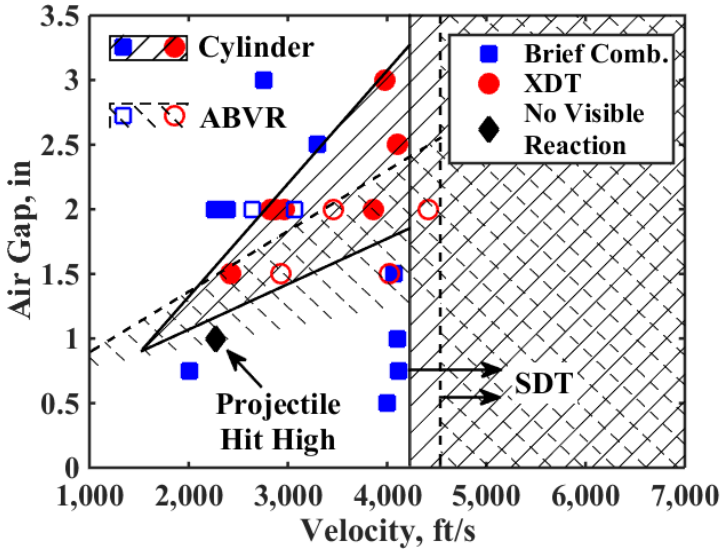

(b)

Figure 5 Different detonation reactions as a function of fragment velocity and air gap for a web thickness of (a) 1.25 in (ABVR) and 1.09 in (cylindrical) or (b) 2.50 in (ABVR) and 2.34 in (cylindrical). Lined regions are where detonations occur.

The discrepancy between the XDT reaction region for the 2.50/2.34 in web thickness ABVR and cylindrical sections is most likely caused by the introduction of the

curved surface. The curvature likely allows the fragment to interact with more propellant as it passes through, as noted by Finnegan et al. This would cause more propellant to enter the propellant cloud, decreasing its porosity. Thus, cylindrical sections would require larger air gaps to obtain the correct porosity for XDT to occur and would be able to sustain an XDT reaction at even larger air gaps. It is likely that this also occurs for the thinner 1.25/1.09 thick samples, but the change in XDT limits must be less than the resolution of obtained data points.

ABVR VS. ANALOG MOTOR

The analog motor was designed based off the results obtained with the ABVR and cylindrical experiments. If those experiments were somewhat representative in predicting how a full scale motor would react, then the analog motor would have detonations nearing as low as 2700 ft/s, a velocity most would not have considered unlikely given fragment impact testing on motors with similar propellant. Furthermore, such a velocity would be very concerning, as statutory requirements indicate motors must pass fragment impact tests without detonating at a velocity over three times this velocity. In order to investigate the different detonation mechanisms and if the ABVR experiment is potentially representative of a full scale motor, six analog motors were impacted with FSP's at velocities near the different reaction thresholds identified in the previous experiments.

A comparison of SDT thresholds and XDT reaction regions for ABVR, cylindrical, and analog motor is provided in Figure 6. The SDT velocity threshold for the analog motor was found to be 4675 ± 118, 139 ft/s higher than the ABVR experiment. Accounting for the ± range of the SDT thresholds, it is possible that the difference between the ABVR experiment and the analog motor is even less than what is reported. The lowest velocity a detonation (XDT) occurred at was 2538 ft/s, resulting in a large fireball, see Figure 7, and pressures over 550 psi at 5 ft from the motor and 280 psi at 10 ft. This resulted in an XDT threshold velocity which was about 1000 ft/s slower than what was found in the ABVR experiments. Again, this is likely due to the curvature of analog motor and the resulting differences in the propellant cloud porosity. Despite this somewhat notable discrepancy, the ABVR experiment was quite valuable in identifying regions where detonations could occur at much lower velocities than would previously would have been suspected.

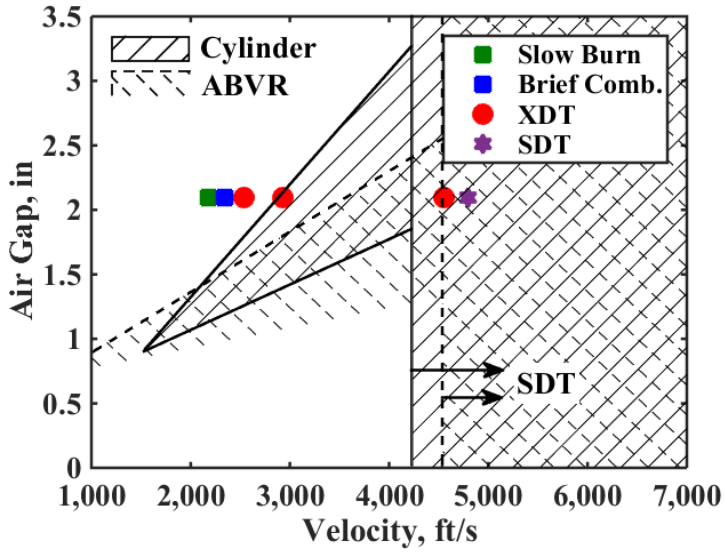

Figure 6 Data obtained for the analog motor compared to the SDT threshold and XDT reaction regions for the ABVR (2.50 in web thickness) and cylinder (2.34 in web thickness) experiments. Lined regions are where detonations occur.

(a) (b)

Figure 7 The test article (a) before the e fragment impacted, and (b) the detonative response that followed after impact.

While the ABVR experiment appears to be a reasonable sub-scale test in predicting the detonative response of full scale motors, it is unclear on how well it is at predicting a non-detonative response for nitramine-based propellants. In the ABVR experiment, if a detonation did not occur, a brief combustion event would produce varying amounts of pressure (under 10 psi) and do little to no damage to the wooden table it was placed upon. In full-scale motor tests, explosions, burns, and brief combustion events have all been observed, and there is no apparent direct correlation between those tests and the amount of pressure or damage observed in the ABVR experiments. The only correlation that could be noteworthy is that the higher the pressure output observed in the ABVR experiments, the greater the violence observed in full scale motor tests; however, there is not enough data available to correlate those pressures to distinct reaction zones/mechanisms. Thus, it appears that the current ABVR experiment may be better suited to investigate detonative responses.

SUMMARY AND CONCLUSIONS

The ABVR experiments identified several regions, dependent of fragment velocity and air gap, where either SDT or XDT reactions would occur. These regions changed as propellant thickness and casing materials were changed. Similar reaction regions were observed when changing from ABVR to cylindrical experiments. For samples that had a propellant thickness of 1.09/1.25 in, both XDT and SDT regions were nearly identical, see Figure 5 (a). However, a measureable deviation was observed for the XDT regions when the propellant thickness was increased to 2.34/2.50 in, see Figure 5 (b). It is likely that this discrepancy is a result of more material entering the propellant cloud for the cylindrical samples, causing its porosity to differ from the propellant cloud produced in the planar ABVR experiments. Similar deviations were observed when comparing the reaction response of the analog motor and what was observed in the ABVR experiment (see Figure 6). The SDT thresholds were very similar, but the XDT reaction regions were measurably different.

ACKNOWLEDGMENTS

The authors would like to thank Bradley White and Keo Springer of Lawrence Livermore National Laboratory, Eric Harstad of Sandia National Laboratories, and Tom Mason of Los Alamos National Laboratory for their suggestions and input. They would like to recognize David Huebner, Joey Reed, William Delaney, Ray Klaver and Zachary Hoernschemeyer for their support in performing experiments. Finally, they would like to thank the Joint Insensitive Munitions Technical Program for the financial support to perform these efforts (Task 15-2-74).

REFERENCES

1. Finnegan, S. A., Pringle, J. K., Schulz, J. C., Heimdahl, O. E. R., and Lindfors, A. J., **Impact-Induced Delayed Detonation in an Energetic Material Debris Bubble Formed at an Air Gap**, International Journal of Impact Engineering, Vol. 14, pp. 241-254, 1993.
2. Finnegan, S. A., Pringle, J. K., Atwood, A. I., Heimdahl, O. E. R., and Covino, J., **Characterization of Impact-Induced Violent Reaction Behavior in Solid Rocket Motors Using a Planar Motor Test Model**, International Journal of Impact Engineering, Vol. 17, pp. 311-322, 1995.
3. Haskins, P. J., Cook, M. D., and Cheese, P. J., **Studies of XDT Phenomena Under Fragment Attack Impact Conditions**, Science and Technology of Energetic Materials, Vol. 66, 2005.
4. Haskins, P. J., and Cook, M. D., **On Delayed Detonation (XDT) Under Fragment Impact – An Analysis Of Experimental Data and a Simple Phenomenological Model**, AIP Conference Proceedings, Nashville, TN, June 28-July 3, 2009.
5. Pfeil, M. A., Stanfield, J. A., Neidert, J. B., Harstad, E. N., White, B. W., and Springer, H. K., **Parameters Influencing the Response of MSP-1 Propellant Subject to Fragment Impact**, NDIA IMEM, Nashville, TN, Sept. 12-15, 2016.